Bulgarian Chemical Communications, Volume 47, Special issue C (pp. 19–24) 2015

Redox properties of ceria-alumina oxides

R. Palcheva[1], B. Pawelec[2], E. Gaigneaux[3], J. L. Fierro[2], S. Damyanova[1]*

[1]*Institute of Catalysis, Bulgarian Academy of Sciences, G. Bonchev St., Bldg. 11, 1113 Sofia, Bulgaria*
[2]*Instituto de Catálisis y Petroleoquímica, CSIC, Cantoblanco, 28049 Madrid, Spain*
[3]*Université Cathlolique de Louvain, Institute of Matter Condensed and Nanosciences (IMCN), Molecules, Solids and Reactivity (MOST), Croix du Sud, 2/L17.05.17, B-1348 Louvain la Neuve, Belgium*

Received 15 October 2015; Revised 4 November 2015

A series of $x$$CeO_2$-$Al_2O_3$ samples of different CeO_2 loading (x = 1–12 wt.%) were prepared by impregnation of γ-alumina with aqueous solution of $(NH_4)_3[Ce(NO_3)_6]$. The effect of CeO_2 content on the structure, textural and redox properties of $x$$CeO_2$-$Al_2O_3$ samples was studied by using N_2 adsorption-desorption isotherms, XRD, and TPR. It was shown that the increase of CeO_2 content leads to a decrease in surface area and pore volume of mixed oxides caused by filling the pores with cerium oxide particles. XRD measurements detected an increase of CeO_2 average particle size on increasing ceria content. The redox properties of $x$$CeO_2$-$Al_2O_3$ oxides were modified by a consecutive reduction and oxidation treatment, which was more evident for 6- and 12-wt.% CeO_2 samples. An enhanced reducibility upon reduction-oxidation treatment of $x$$CeO_2$-$Al_2O_3$ oxides was revealed by formation of a phase of high oxygen mobility reduced at a lower temperature.

Key words: mixed CeO_2-Al_2O_3 oxides, redox properties, XRD, TPR.

INTRODUCTION

Cerium(IV) oxide and CeO_2-containing materials have a great importance as catalysts and as structural and electronic promoters in catalysts for different heterogeneous catalytic reactions. The CeO_2-Al_2O_3 system is of special interest in catalysis because of its technological importance in auto exhaust catalysis [1, 2], in reforming processes of ethanol and methane to hydrogen production [3, 4], or in water-gas shift reaction and selective CO oxidation in the presence of a large excess of hydrogen (PROX) [5]. In spite of the great importance of ceria as an active catalyst component, a more detailed mechanistic understanding on how cerium affects catalytic processes is still a matter of considerable debate, although some key findings are well established.

Several works have been devoted to studies of the physical and chemical features of ceria deposited on Al_2O_3, with the aim of improving ceria properties through a better knowledge of the nature of interaction between CeO_2 and Al_2O_3. Some authors believe that the structural and morphological modifications operated by ceria on Al_2O_3 play a minor role in relation to chemical effects as modification of acid-base properties, which is much more important for determineing the properties of the system. Other authors proposed that the stabilization effect of ceria in terms of modification of the structural and textural features of alumina is a major factor [1, 6]. Usually, these discrepancies may originate from different experimental conditions that are employed in the studies, such as temperature range investigated, durability of thermal treatment and pretreatment as well as use of some additional promoters.

One of the most important beneficial effects of ceria is the ability to oxidize deposited carbon species over catalytic metal centres and to increase catalyst stability due to its high oxygen storage capacity (OSC) caused by the redox couple $Ce^{4+} \leftrightarrow Ce^{3+}$ under oxidation and reduction conditions [7, 8]. Nanostructured mixed metal oxides supported on alumina have been prepared by impregnation of γ-Al_2O_3 with cerium/zirconium citrate solutions, which exhibit a high OSC [8]. It was shown [10] that the following types of cerium oxides as CeO_2, CeO_{2-x}/Al_2O_3, and $CeAlO_3/Al_2O_3$ exhibit a decrease of OSC value in the order: finely-divided CeO_{2-x} > $CeAlO_3$ > small-sized CeO_2 > large CeO_2 crystallites.

To improve catalyst performance, further knowledge of the interaction between ceria and alumina in mixed CeO_2-Al_2O_3 oxides is essential, because they are potential carriers for supported Ni catalysts for ethanol or methane reforming to hydrogen. In the present work, it was attempted to investigate the effect of CeO_2 content on the structure and reductive properties of mixed $x$$CeO_2$-$Al_2O_3$ oxides by using different techniques: N_2 adsorption-desorption iso-

* To whom all correspondence should be sent:
E-mail: soniad@ic.bas.bg

therms, X-ray diffraction (XRD) and temperature programmed reduction (TPR). Studies related to subjecting mixed CeO_2-Al_2O_3 oxides to consecutive reducing and oxidizing conditions at different reoxidation temperatures were performed.

EXPERIMENTAL

Sample preparation

CeO_2-Al_2O_3 supports were obtained by impregnation of γ-Al_2O_3 (Topsøe) with an aqueous solution of $(NH_4)_3[Ce(NO_3)_6]$, a 99.99% product of Degussa, with an appropriate concentration of CeO_2. The solution with alumina was stirred at 50°C for 4 h and after that the water was evaporated by a Rotavapor. The obtained samples were dried in air at 100°C for 12 h and calcined at 600°C for 4 h. Nominal CeO_2 content was in the range of 1–12 wt.%. The samples were denoted as xCe-Al, where x is the theoretical amount of CeO_2. For comparative purposes, ceria was obtained by calcination of $(NH_4)_3[Ce(NO_3)_6]$ in air at 650°C for 2 h.

Methsods

N_2 adsorption-desorption isotherms of calcined samples were recorded at 77 K on a Micromeritics TriStar 3000 apparatus. Beforehand the samples were outgassed at 150°C for 24 h under vacuum (10^{-4} mbar) to obtain a relatively clean surface. Specific surface area (S_{BET}), pore volume (V_p), and average pore diameter (D_p) of $x$$CeO_2$-$Al_2O_3$ samples were evaluated from the N_2 adsorption-desorption isotherms. Surface area were calculated according to the BET method using nitrogen adsorption data taken in the relative equilibrium pressure interval of $0.03 < P/P_0 < 0.3$.

XRD analysis was performed in 2θ range between 10 and 90° by a computerized Seifert 3000 diffractometer, using Ni-filtered CuKα (λ = 0.15406 nm) radiation and a PW 2200 Bragg-Brentano θ/2θ goniometer equipped with a bent graphite monochromator and an automatic slit. A step size of 0.02 and a step scan of 2 s were used to identify samples structure. Phase identification was carried out by comparison with JCPDF database cards. CeO_2 average crystallite size was estimated by Debye-Scherrer equation using the X-ray diffraction pattern at 2θ = 28.8°.

TPR experiments were conducted on a Micromeritics TPD/TPR 2900 equipment provided with a TCD and interfaced to a data station. Samples of 0.100 g were reduced in a flowing gas containing 10 vol.% H_2 in Ar up to a final temperature of 1000°C at a total flow rate of 50 ml.min^{-1} and heating rate of 15 deg.min^{-1}. The samples were subjected to redox treatment at 500°C (R-O_{500}) and 700°C (R-O_{700}), which involved H_2-TPR to 1000°C followed by cooling to 500°C/700°C under argon and *in situ* oxidation by an oxygen flow (70 ml.min^{-1}) at 500°C/700°C for 2 h. After each oxidation run, the reactor was cooled to r.t. in Ar flow and the samples were subjected to TPR (from r.t. to 1000°C).

RESULTS AND DISCUSSION

Textural properties and structure

N_2 adsorption-desorption isotherms of calcined $x$$CeO_2$-$Al_2O_3$ samples of different CeO_2 content shown in figure 1 have hysteresis loops that belong to H1 type according to IUPAC, typical for mesoporous materials [11]. Textural characteristics of the samples are given in Table 1.

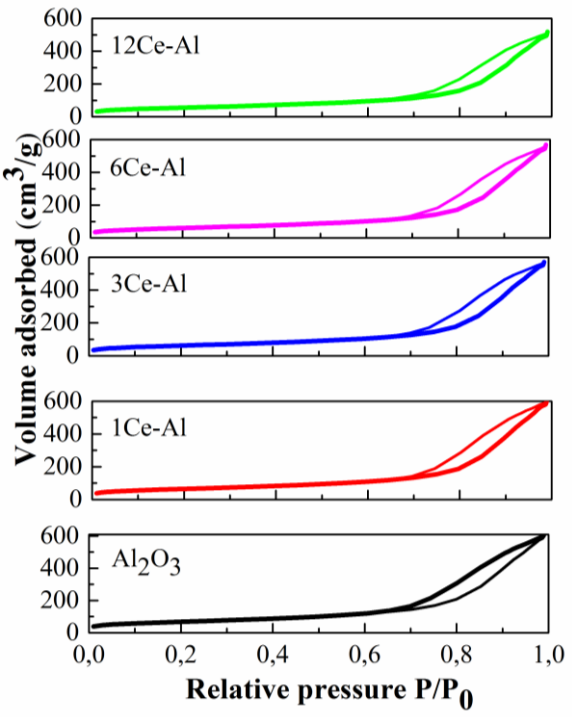

Fig. 1. N_2 adsorption-desorption isotherms of γ-Al_2O_3, bulk CeO_2, and mixed $x$$CeO_2$-$Al_2O_3$ oxides of different CeO_2 content.

Introduction of small amount of CeO_2 (1 wt.%) to alumina led to a slight decrease of the S_{BET}. However, increasing the CeO_2 content to 12 wt.% causes a significant decrease in S_{BET} and V_p. Lower surface area and pore volume values of $x$$CeO_2$-$Al_2O_3$ oxides compared to those of alumina can be related to a blockage of alumina pores by cerium oxide species [12] due to easy-going agglomeration of CeO_2 over alumina. In addition, ceria agglomeration may develop some porosity, which contributes to measured

textural properties [13]. The mean pore diameter of xCeO$_2$-Al$_2$O$_3$ samples is higher than that of alumina (Table 1). This is probably caused by the presence of particles with larger pores and possible blockage of small diameter pores by cerium oxide species.

Table 1. Textural properties and particle size (D_{XRD}) of CeO$_2$-Al$_2$O$_3$ oxides

Samples	S_{BET} ($m^2.g^{-1}$)	V_p ($cm^3.g^{-1}$)	Pore diameter (nm)	D_{XRD} (nm)
Al$_2$O$_3$	248	0.92	14.6	–
1Ce-Al	228	0.91	15.7	–
3Ce-Al	217	0.87	15.7	5.3
6Ce-Al	213	0.86	15.7	7.2
12Ce-Al	198	0.79	15.4	9.2

XRD patterns of Al$_2$O$_3$ and calcined xCeO$_2$-Al$_2$O$_3$ oxides of different CeO$_2$ content are shown in figure 2. For comparison, XRD data on bulk CeO$_2$ is also included. The XRD patterns indicate that all CeO$_2$-containing samples demonstrate peaks at 2θ = 28.8, 32.6, 47.4, 56.1, and 76.5° characteristic of a CeO$_2$ phase with fluorite structure (JCPDS 34-0394). These peaks become more intense on increasing the ceria content in xCeO$_2$-Al$_2$O$_3$ samples. CeO$_2$ average crystallite size (D_{XRD}) increases from 5.3 nm to 9.2 nm for 1- and 12-wt.% CeO$_2$ samples, respectively (Table 1). Reflections at 2θ = 33.4, 37.6, 40.5, 45.8, and 67.1° (JCPDS 10-425) are assigned to γ-Al$_2$O$_3$. The intensity of the main line of alumina support (2θ = 67.1°) decreases upon increasing cerium oxide loading, which is most visible with 12 wt.% CeO$_2$. This could be explained by existence of some interaction between cerium and aluminium or increased coverage of CeO$_2$ crystallites on alumina. Ferreira *et al.* [14] observed a small amount of cerium oxide species at low CeO$_2$ content (x ≤ 3 wt.%), which interacts with the alumina support surface to form non-stoichiometric CeO$_{2-x}$.

TPR and redox properties

TPR profiles of bulk CeO$_2$ and calcined xCeO$_2$-Al$_2$O$_3$ samples, and effects of subsequent oxidation and reduction cycles are compared in figure 3. The TPR shape of bulk CeO$_2$ is very similar to that reported in the literature and it can be interpreted as a stepwise reduction process. Bulk CeO$_2$ manifests two well-known peaks [15]: a small peak at about 508°C and a large peak at 749°C. The low-temperature peak is due to reduction of most easily reducible surface capping oxygen of CeO$_2$, while removal of bulk oxygen is registered by the high-temperature TPR pattern. A good correlation between surface area and H$_2$ consumption of the first peaks has been found [16]. Variations between surface area and H$_2$ consumption are linear indicating that at first ceria reduction occurs on the surface and then progressively affects the bulk. Thus, the initial progress of reduction is highly sensitive to the surface area and bulk reduction, favoured by high oxygen mobility in the CeO$_2$ lattice, is beginning when all surface sites are fully reduced. The low-temperature peak is due to reduction of readily reduced surface capping oxygen of CeO$_2$ followed by generation of vacancies and surface Ce^{3+} ions, which can easily be oxidized to Ce^{4+} under oxidation conditions [17]. At the second step, the reduction process is associated with creation of oxygen vacancies in the bulk of CeO$_2$. Therefore, the high temperature peak at 749°C can be attributed to complete reduction of Ce^{4+} to Ce^{3+} by removing O^{2-} anions of the ceria lattice and formation of Ce$_2$O$_3$. Due to low surface area of the bulk CeO$_2$ sample (18 $m^2.g^{-1}$) prepared by decomposition of $(NH_4)_3[Ce(NO_3)_6]$, the low-temperature signal is very weak, and the majority of hydrogen consumption originates from the reduction of large ceria crystallites (Fig. 3).

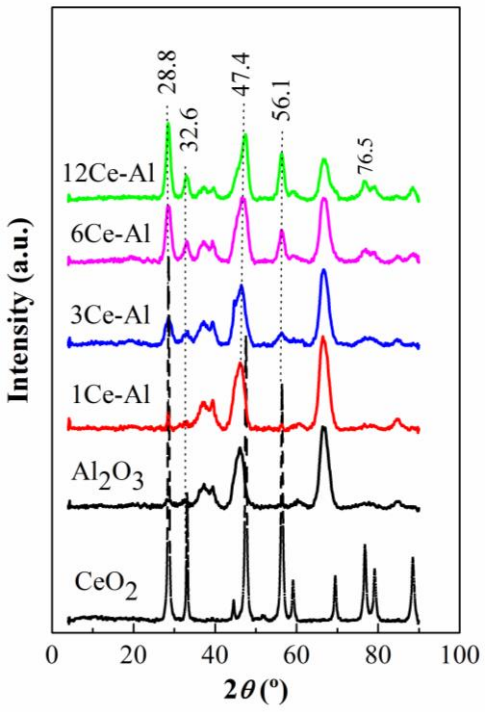

Fig. 2. XRD of bulk CeO$_2$ and mixed xCeO$_2$-Al$_2$O$_3$ oxides of different CeO$_2$ content.

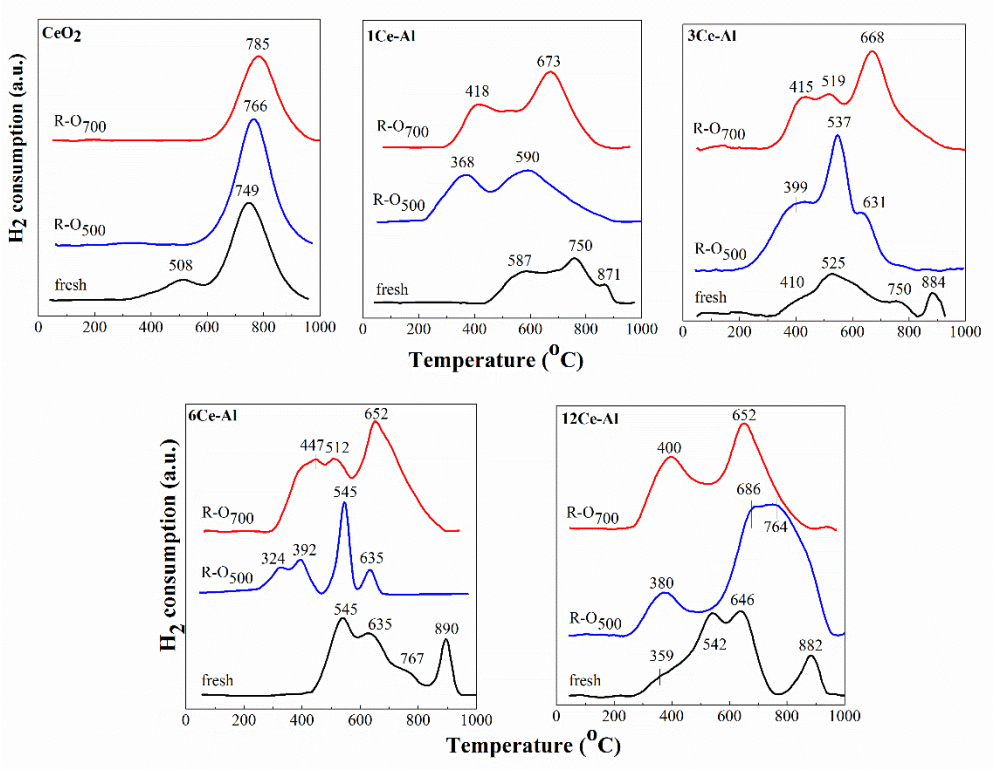

Fig. 3. TPR of bulk CeO_2 and mixed $xCeO_2$-Al_2O_3 oxides subjected to R-O_{500} and R-O_{700}.

As was previously discussed [18], surface and bulk reduction cannot easily be distinguished by the conventional TPR technique, since both processes occur almost simultaneously during the TPR experiment. As can be seen in Fig. 3, reductive behaviour of alumina-supported CeO_2 of different concentration is modified depending on the extent and nature of interaction between ceria and alumina. The TPR profiles of mixed $xCeO_2$-Al_2O_3 oxides show new characteristics: (i) TPR peak shape depends on crystallite size of deposited CeO_2; (ii) significant shifts of peak temperatures are apparent; (iii) apparent H_2 consumption continues even after the main peaks characteristic of bulk ceria; (iv) low temperature features, assigned to surface oxygen reduction, fall in a wide temperature range, and (v) effectiveness of Ce^{4+} reduction increases upon increasing CeO_2 loading at all reduction temperatures, as revealed by an increase of peak intensity.

Regardless of CeO_2 loading, the TPR profiles of calcined $xCeO_2$-Al_2O_3 samples can be divided into three temperature regions: region I (200–500°C), region II (500–800°C), and region III (> 800°C) (Fig. 3). Region I peaks are generally associated with reduction of small ceria crystallites and/or surface cerium oxide species weakly interacting with support, whereas region II is ascribed to reduction of large/bulk CeO_2 crystallites or cerium oxide species or cerium atoms that interact strongly with alumina [19]. A high-temperature peak at 882–890°C observed with all samples may be caused by formation of surface $CeAlO_3$ species associated with Ce^{4+} reduction to Ce^{3+}. It has been shown [20, 21] that, depending on ceria loading, ceria reduction on alumina under hydrogen involves at least two reactions: formation of non-stoichiometric cerium oxides and cerium aluminate ($CeAlO_3$). It should be noted that an increase in $CeAlO_3$ peak intensity is accompanied by a decrease in high-temperature peak intensity due to bulk ceria reduction (Fig. 3).

TPR profiles of fresh CeO_2 samples of ≥ 3-wt.% content show features in the low-temperature region (< 500°C) due to well dispersed very small ceria particles on alumina surface (Fig. 3). However, there is still reduction of large CeO_2 crystallites of different size in the profile of 12-wt.% CeO_2 sample as revealed by peaks at 542 and 640°C. Shifting of reduction peaks to low temperatures is in agreement with a suggestion that a high concentration of ions of redox character (i.e. Ce^{4+} ions) favours an electron transfer as $Ce^{4+} \leftrightarrow Ce^{3+}$. Prevailing peaks in the TPR profile of a sample of the lowest CeO_2 content (1 wt.%) in the medium temperature range may be mainly caused by reduction of cerium oxide species that interacts strongly with alumina due to high ceria dispersion. The lowest intensity of the $CeAlO_3$ peak at 882°C is due to the smallest number of cerium oxide species in $1CeO_2$-Al_2O_3.

After R-O_{500} and R-O_{700} treatment of bulk CeO_2 the small peak caused by surface shell reduction of

CeO_2 disappeared, while the peak due to bulk reduction of ceria was shifted to higher temperatures (from 749°C for fresh samples to 766 and 785°C for R-O_{500} and R-O_{700}, respectively).

The TPR profiles of all $x CeO_2$-Al_2O_3 samples of different CeO_2 content subjected to R-O_{500} show a marked enhancement of low-temperature reducibility relative to that of fresh samples (Fig. 3). Improved low-temperature reducibility was observed for a mixed oxide of 6 wt.% expressed by a small peak at a lower temperature of 324°C, probably due to formation of a small fraction of non-stoichiometric cerium oxides species. Regardless of CeO_2 loading, some agglomeration of cerium oxide species was observed after R-O_{500} treatment, as revealed by the peaks in the 537–590°C range. On the other hand, one cannot exclude a partial segregation of species of low oxidation state, such as Ce^{3+}, on the ceria surface owing to the higher ionic radius of Ce^{3+} (1.1 Å) compared to that of Ce^{4+} (0.97 Å) [22]. Thus, segregation may lead to complete disappearance of the peak characteristic of $CeAlO_3$ in the TPR profiles of all samples. It is well known [21] that well dispersed CeO_x entities can be precursors for surface $CeAlO_3$ formation under reduction, while they are readily transferred to CeO_2 after oxidation.

However, some distinct features characterize the TPR profile of the sample of the highest CeO_2 loading (12 wt.%). Besides the presence of small well-dispersed ceria particles, a broad high intensity peak in the high temperature region between 600 and 900°C was observed attributed to reduction of large CeO_2 crystallites. This indicates that reoxidation at 500°C affects ceria crystallites size in the $12CeO_2$-Al_2O_3 sample, although there is still a fraction of highly reducible ceria in low-loaded samples (Fig. 3).

Subjecting the R-O_{500} samples to R-O_{700} leads to a shift of the TPR peaks to higher temperatures (Fig. 3), which could mean that the average oxidation state in non-stoichiometric ceria approaches +4. The low-temperature peak maxima are almost identical for all oxides, while the higher temperature peaks are shifted to lower values due to bulk ceria reduction detected for high-loaded ceria samples (6 and 12 wt.%) caused by a higher oxygen mobility.

CONCLUSIONS

TPR analysis showed that hydrogen uptake for mixed CeO_2-Al_2O_3 samples is dependent on reoxidation temperature and CeO_2 content. It can be assumed that the amount of initially present cerium in a lower oxidation state formed during sample preparation is higher for samples of lower CeO_2 loading, where the stability of non-stoichiometric ceria is higher. This is in agreement with a lower average size of CeO_2 crystallites of fluorite type structure. Partially reduced cerium oxide entities can be precursors for surface $CeAlO_3$ formation under reduction conditions, the amount being increased upon increasing the CeO_2 content. However, increasing the reoxidation temperature led to disappearance of the surface $CeAlO_3$ due to agglomeration of the cerium oxide species. A higher oxygen mobility was observed for samples of high CeO_2 content (6 and 12 wt.%) due to agglomeration of ceria particles.

***Acknowledgments**: The authors kindly acknowledge financial support by the Bulgarian Science Fund through project FNI E02/16 as well as by bilateral collaborations of the Institute of Catalysis with Catholic University of Louvain la Neuve (Belgium) and Institute of Catalysis and Petrochemistry, Madrid (Spain).*

REFERENCES

1. M. Ozawa, M. Kimura, *J. Mater. Sci. Lett*., **9**, 291 (1990).
2. A. Holmgren, B. Andersson, D. Duprez, *Appl. Catal. B: Environ.*, **22**, 215 (1999).
3. A. C. S. F. Santos, S. Damyanova, G. N. R. Teixeira, L. V. Mattos, F. B. Noronha, F. B. Passos, J. M. C. Bueno, *Appl. Catal. A: Gen*., **290**, 123 (2005).
4. L. S. F. Feio, C. E. Hori, S. Damyanova, F. B. Noronha, W. H. Cassinelli, C. M. P. Marques, J. M. C. Bueno, *Appl. Catal. A: Gen*., **316**, 107 (2006).
5. L. Ilieva, T. Tabakova, G. Pantaleo , I. Ivanov, R. Zanella, D. Paneva, N. Velinov, J. W. Sobczak, W. Lisowski, G. Avdeev, A. M. Venezia, *Appl. Catal A: Gen*., **467**, 76 (2013).
6. A. Piras, A. Trovarelli, G. Dolcetti, *Appl. Catal.* B*: Environ*., **28**, L77 (2000).
7. S. Bose, Y. Wu, *J. Am. Ceram. Soc*., **88**, 1999 (2005).
8. D. Andreeva, R. Nedyalkova, L. Ilieva, M. Abrashev, *Appl. Catal. B: Environ*., **52**, 157 (2004).
9. R. Di Monte, P. Fornasiero, J. Kaspar, M. Graziani, *Stud. Surf. Sci. Catal*., **140**, 229 (2001).
10. M. Haneda, T. Mizushima, N. Kakuta, A. Ueno, Y. Sato, S. Matsuura, K. Kasahara, M. Sato, *Bull. Chem. Soc. Jpn*., **66**, 1279 (1993).
11. G. Leofanti, M. Padovan, G. Tozzola, B. Venturelli, *Catal. Today*, **41**, 207 (1998).
12. C. Morterra, G. Magnacca, V. Bolis, G. Gerrato, M. Baricco, A. Giachello, M. Fucale, *Stud. Surf. Sci. Catal*., **96**, 361 (1995).
13. V. B. Mortola, S. Damyanova, D. Zanchet, J. M. C. Bueno, *Appl. Catal. B: Environ*., **107**, 221 (2011).
14. A. P. Ferreira, D. Zanchet, J. C. S. Araujo, J. W. C. Liberatori, E. F. Souza-Aguiar, F. B. Noronha, J. M. C. Bueno, *J. Catal*., **263**,335 (2009).
15. H. C. Yao, Y. F. Yu Yao, *J. Catal*., **86**, 254 (1984).

16. V. Perrichon, A. Laachir, G. Beregeret, R. Frety, L. Tounayan, *J. Chem. Soc., Faraday Trans*., **90,** 773 (1994).
17. G. Jacobs, U. M. Graham, E. Chenu, P. M. Patterson, A. Dozier, B. A. Davis, *J. Catal*. **229**, 499 (2005).
18. G. Balducci, J. Kaspar, P. Fornasiero, M. Graziani, M. S. *Islam, J. Phys. Chem. B*, **102**, 557 1998.
19. F. Giordano, A. Trovarelli, C. de Leitenburg, M. Giona, *J. Catal.*, **193**, 273, (2000).
20. S. Geller, P. M. Raccah, *Phys. Rev. B,* **2**, 1167 (1970).
21. A. Piras, S. Colussi, A. Trovarelli, V. Sergo, J. Llorca, R. Psaro, L. Sordelli, *J. Phys. Chem. B*, **109**, 11110 (2005).
22. A. I. Kozlov, D. H. Kim, A. Yezerets, P. Andersen, H. H. Kung, M. C. Kung, *J. Catal*., **209**, 417 (2002).

ОКИСЛИТЕЛНО-РЕДУКЦИОННИ СВОЙСТВА НА CeO_2-Al_2O_3 ОКСИДИ

Р. Палчева[1], Б. Павелец[2], Е. Геньо[3], Х. Л. Г. Фиеро[2], С. Дамянова[1]*

[1] *Институт по катализ, Българска академия на науките, 1113 София, България*
[2] *Институт по катализ и нефтохимия, Кантобланко, 28049 Мадрид, Испания*
[3] *Католически университет на Льовен, B-1348 Льовен-ла-Ньов, Белгия*

Постъпила на 15 октомври 2015 г.; Преработена на 4 ноември 2015 г.

(Резюме)

Получени са $x$$CeO_2$-$Al_2O_3$ оксиди с различно съдържание на CeO_2 (x = 1–12 тегл.%) чрез импрегниране на γ-Al_2O_3 с воден разтвор на $(NH_4)_3[Ce(NO_3)_6]$. Ефектът на съдържанието на CeO_2 върху структура, текстура и окислително-редукционни свойства на $x$$CeO_2$-$Al_2O_3$ образци с помощта на адсорбционно-десорбционни изотерми на азот, рентгенова дифракционна спектроскопия (РДС) и температурно-програмирана редукция (ТПР). Показано е, че средният размер на частиците на CeO_2 на повърхността на γ-Al_2O_3 нараства с увеличаване на концентрацията му. Окислително-редукционните свойства на $x$$CeO_2$-$Al_2O_3$ са модифицирани чрез последователна обработка в редукционни и окислителни условия, което е по-ярко забележимо за образци с 6 и 12 тегл.% CeO_2. Повишената редуцируемост на образците при окислително-редукционното им третиране се проявява чрез образуването на фаза, редуцираща се при по-ниска температура, което се дължи на по-високата мобилност на кислорода.